http://www.scirp.org/journal/jbise

J. Biomedical Science and Engineering, 2018, Vol. 11, (No. 12), pp: 338-347

Vibration Signal Analysis for Detecting Early-Stage Lumbar Spondylolysis Using Synthetic Bone

Hiroyuki Watanabe[1], Naohiro Tahara[2], Rina Sakai[3], Naonobu Takahira[1], Suguru Torii[4], Atsuhiko Matsunaga[1]

[1]Department of Rehabilitation, School of Allied Health Sciences, Kitasato University, Sagamihara, Japan; [2]Osada Hospital, Yokohama, Japan; [3]Department of Medical Engineering and Technology, School of Allied Health Sciences, Kitasato University, Sagamihara, Japan; [4]Faculty of Sports Science, Waseda University, Tokorozawa, Japan

Correspondence to: Hiroyuki Watanabe, hw@ahs.kitasato-u.ac.jp

Keywords: Vibration Signal, Spondylolysis, Synthetic Bone, Lumbar Vertebra

Received: November 13, 2018 **Accepted:** December 25, 2018 **Published:** December 28, 2018

ABSTRACT

Bone fractures can be detected by analyzing vibration signals following bone stimulation. This method can also be applied to detect stress fractures, such as spondylolysis. The aim of this study was to investigate whether vibration signal analysis can be used to detect lumbar spondylolysis in synthetic bone. Four synthetic spondylolysis models of the fifth lumbar vertebra (Sawbones, product No. SAW1352-10: Malmö, Sweden) were prepared, with the following conditions: intact, unilateral defect, and bilateral defect. Unilateral defects were created by making an incision of either half the diameter (50% incision) or the entire diameter (100% incision) in length through the pars interarticularis or pedicle. Bilateral defects were created by making an additional incision of half the diameter in length on the opposite side of the defected pars interarticularis or pedicle (50% + 100% incision). Hammering was performed five times on each spinous process of the fixed synthetic bones and vibration signals were measured using an accelerometer attached to the contralateral side of the hammer. Signals were analyzed using fast Fourier transform. The parameters analyzed included the mean power frequency, first power minimum frequency (the minimum value between the first and second peaks), spectral areas of low and high frequency bands, and the relative ratio between the spectral areas of low and high frequency bands. The relative ratio was significantly lower in the 50%, 100%, and 50% + 100% incision conditions compared to the intact condition ($p < 0.01$), suggesting the potential utility of vibration signal analysis in diagnosing lumbar spondylolysis.

1. INTRODUCTION

Lumbar spondylolysis is a fatigue fracture of the vertebral pars interarticularis caused by repeated extension and rotation of the lower trunk in young athletes [1-3]. The prevalence of pars defects is reportedly high in adolescent athletes with back pain [4-7]. In particular, bilateral lumbar spondylolysis will be an onset of spondylolisthesis in the future, and may eventually progress to lumbago [8, 9]. Although lumbar spondylolysis is a major cause of low back pain in adolescence, it is usually asymptomatic in early stages. Bony healing is more likely to occur when spondylolysis is diagnosed within one month of symptom onset, with unilateral fractures having higher healing rates than bilateral or pseudo-bilateral fractures [8]. On the other hand, if bone healing cannot be achieved, athletes with lumbar spondylolysis may develop low back pain and/or spondylolisthesis in the future. For these reasons, early detection of lumbar spondylolysis is important for adolescent athletes.

Recently, the use of CT and MRI with high detection capability has enabled the early diagnosis of lumbar spondylolysis [10, 11]. In particular, early-stage lumbar spondylolysis can be detected by high intensity signals on STIR in MRI [12]. However, since the predominant clinical manifestation of lumbar spondylolysis is localized pain, patients with early-stage lumbar spondylolysis are less likely to undergo MRI examination at medical institutions.

Vibration signal analysis is a method used to measure changes in specific signal frequency components resulting from bone fracture, as the natural frequency of bone varies depending on bone shape [13]. Unlike large-size imaging systems, such as MRI and CT, vibration signal analysis only requires simple equipment and can be performed anywhere. Thus, it can be performed outside medical institutions, where imaging examinations cannot be carried out. To detect early-stage spondylolysis using the vibration signal analysis is possible to prevent aggravation of spondylolysis as a new diagnostic tool instead of the imaging systems. This study aimed to investigate whether vibration signal analysis can be used to detect lumbar spondylolysis in synthetic bone.

2. METHODS

Lumbar spondylolysis models were created by artificial processing using a synthetic fifth lumbar vertebra (Sawbones, product No. SAW1352-10: Malmö, Sweden) (**Figure 1**). Incisions were made on the right or/and left side of the pars interarticularis or pedicle, as follows: incision in the right pars interarticularis (model A), incision in the left pars interarticularis (model B), incision in the right pedicle (model C), and incision in the left pedicle (model D) (**Figure 2**). For each model, the following four conditions were prepared: intact, unilateral defect (50% and 100% incision conditions), and bilateral defect (50% + 100% incision condition). Unilateral defects were created by making an incision of either half the diameter (50% incision) or the entire diameter (100% incision) in length through the pars interarticularis or pedicle. Bilateral defects were created by making an additional incision of half the diameter in length on the opposite side of the defected pars interarticularis or pedicle (50% + 100% incision).

Figure 1. Synthetic fifth lumbar vertebra (Sawbones, product No: SAW1352-10, Malmö, Sweden).

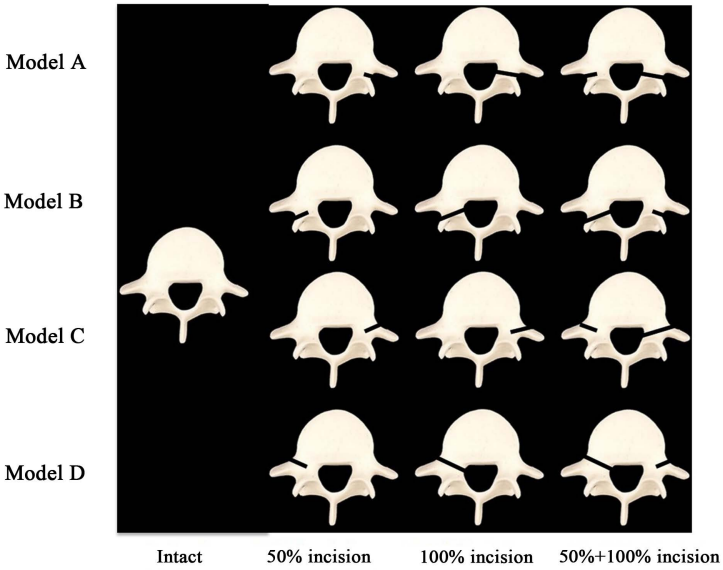

Figure 2. Lumbar spondylolysis models with different incision sides and conditions. Model A: incision in the right pars interarticularis which is behind the transverse process. Model B: incision in the left pars interarticularis which is behind the transverse process. Model C: incision in the right pedicle which is in front of the transverse process. Model D: incision in the left pedicle which is in front of the transverse process. The 50% and 100% incision conditions had an incision of either half the diameter or the entire diameter of pars interarticularis or pedicle. The 50% + 100% incision condition, *i.e.*, the bilateral spondylolysis model, had a combination of 50% and 100% incisions in either the pars interarticularis or pedicle.

The vibration signal analysis system consisted of a high-density polyethylene hummer, uniaxial accelerometer (AS-50B: Kyowa Electronic Instruments Inc., Tokyo), amplifier (DPM-711B: Kyowa Electronic Instruments Inc., Tokyo), analog-to-digital converter (PowerLab: AD instruments Inc., Aichi), and personal computer. The vertebral body of each lumbar spondylolysis model was fixed with a vise, so that the spinous process faced upward (**Figure 3**). Vibration signals were measured using a uniaxial accelerometer (sampling rate, 10 KHz) attached to the contralateral side of the hammer with a high-density polyethylene head. Hammering was performed five times on each spinous process of the fixed models. In all cases, hammering was repeated by a single skilled physical therapist who demonstrated excellent inter-rater reliability, with a mean power frequency of 0.949 in the low-frequency area and 0.911 in the high-frequency area (Cronbach α).

The signals were fast Fourier transformed after filtering of the 6th degree Butter Worth Filter (low pass filter)using MATLAB R2017b (MathWorks Inc., Natick). The following parameters were analyzed: mean power frequency (MPF), first minimum frequency (FMF: It was detected as the minimum value of power between the first and second peaks using MATLAB program.), spectral areas of the low (SAL) and high (SAH) frequency bands, and the relative ratio (RR) of SAL to SAH. SAL indicates the area of the frequency band from the minimum value to the FMF [14, 15]. SAH indicates the area of the frequency band from the FMF to the Nyquist frequency (**Figure 4**).

MPF

Equation (1) was used to calculate the MPF:

$$\mathrm{MPF} = \int_{fL}^{fH} fP(f,t,T)\mathrm{d}f \Big/ \int_{fL}^{fH} P(f,t,T) \tag{1}$$

where T is the data length, f is the frequency, and $P(f,t,T)$ is the power spectral.

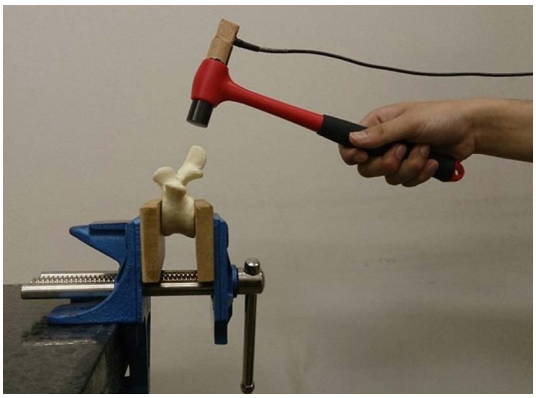

Figure 3. The vertebral body of the lumbar spondylolysis model was fixed with a vise so that the spinous process faced upward. Vibrational signals were measured using a uniaxial accelerometer attached to the contralateral side of the hammer with the high-density polyethylene head.

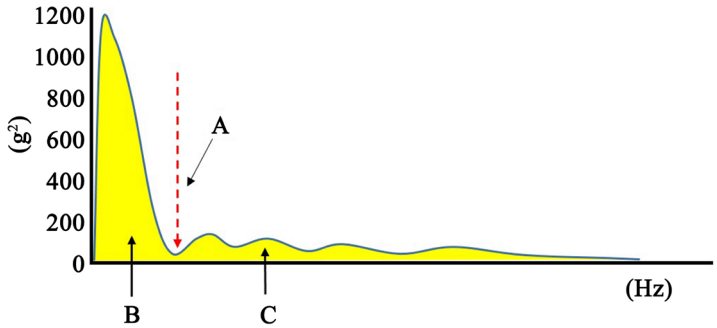

Figure 4. Typical results of FFT vibration signal analysis. A: first minimum frequency (FMF: the minimum value of power between the first and second peaks); B: spectral area of low frequency (SAL); C: spectral area of high frequency (SHL).

SAL

The low spectral area was calculated from the integral value of the band lower than the FMF. Equation (2) was used to calculate the low spectral area:

$$\mathrm{SAL} = \int_0^x P(f,t,T)\,\mathrm{d}f \tag{2}$$

where T is the data length, f is the frequency, $P(f,t,T)$ is the power spectral, and x is the FMF.

SAH

The high spectral area was calculated from the integral value of the band higher than the FMF. Equation (3) was used to calculate the high spectral area:

$$\mathrm{SAH} = \int_x^{fc} P(f,t,T)\,\mathrm{d}f \tag{3}$$

where T is the data length, f is the frequency, $P(f,t,T))$ is the power spectral, x is the FMF, and fc is the Nyquist frequency.

3. STATISTICAL ANALYSIS

Analysis of variance was performed to compare each parameter for each lumbar spondylolysis model. The Bonferroni method was used for post hoc test. $P < 0.01$ was considered statistically significant. All statistical analyses were performed using SPSS Statistics 23.0 J (SPSS, Chicago, IL).

4. RESULTS

MPF (Mean power frequency)

Table 1 and Figure 5(a) show the values of MPF in the intact, 50%, 100%, and 100% + 50% incision conditions for models A, B, C, and D: (model A) 289.3 ± 5.9 Hz, 300.3 ± 6.9 Hz, 480.9 ± 9.2 Hz, 626.8 ± 7.7 Hz; (model B) 258.5 ± 0.8 Hz, 260.5 ± 2.4 Hz, 337.7 ± 8.4 Hz, 341.4 ± 16.7 Hz; (model C) 296.3 ± 0.9 Hz, 301.0 ± 2.2 Hz, 402.3 ± 6.5 Hz, 429.6 ± 7.1 Hz; (model D) 273.3 ± 5.6 Hz, 288.5 ± 7.9 Hz, 440.1 ± 20.2 Hz, 579.5 ± 9.9 Hz. Compared to the intact condition, the values of MPF were significantly higher in the 100% and 100% + 50% incision conditions for all models.

Table 1. Results of each parameter for frequency analysis (mean ± SD).

		Incision conditions of pars interarticularis or pedicle			
		intact	50%	100%	100% + 50%
MPF (Hz)	Model A	289.3 ± 5.9	300.3 ± 6.9	480.9 ± 9.2*	626.8 ± 7.7*
	Model B	258.5 ± 0.8	260.5 ± 2.4	337.7 ± 8.4*	341.4 ± 16.7*
	Model C	296.3 ± 0.9	301.0 ± 2.2	402.3 ± 6.5*	429.6 ± 7.1*
	Model D	273.3 ± 5.6	288.5 ± 7.9	440.1 ± 20.2*	579.5 ± 9.9*
FMF (Hz)	Model A	430.0 ± 11.5	390.0 ± 11.5*	160.0 ± 21.2*	125.0 ± 28.9*
	Model B	380.0 ± 25.8	355.0 ± 10.0	217.5 ± 9.6*	210.0 ± 87.0*
	Model C	430.0 ± 11.5	390.0 ± 20.0*	275.0 ± 10.0*	150.0 ± 11.5*
	Model D	412.5 ± 45.0	285.0 ± 44.3*	215.0 ± 10.0*	127.5 ± 23,6*
SAL (g^2)	Model A	26,816.0 ± 2204.4	21,829.3 ± 1563.0*	10,040.9 ± 759.1*	6759.8 ± 1029.7*
	Model B	23,050.8 ± 765.3	19,500.3 ± 679.4*	11,431.5 ± 1587.3*	10,638.5 ± 978.6*
	Model C	23,427.5 ± 1412.2	23,953.8 ± 2045.7	10,337.5 ± 1246.6*	9518.6 ± 152.8*
	Model D	19,185.8 ± 1136.5	13,626.5 ± 1075.2*	7969.1 ± 580.3*	4500.0 ± 347.9*
SAH (g^2)	Model A	3640.2 ± 402.5	3755.2 ± 326.8	4972.8 ± 163.4*	5124.9 ± 752.3*
	Model B	2844.0 ± 118.1	2738.7 ± 87.3	3417.8 ± 311.7	3084.4 ± 154.8
	Model C	3263.0 ± 268.8	3875.7 ± 213.8*	4580.9 ± 460.5*	4675.9 ± 156.2*
	Model D	2872.1 ± 283.6	2900.5 ± 255.2	3763.4 ± 332.5*	3110.8 ± 323.7
RR (g^2/g^2)	Model A	7.4 ± 0.5	5.8 ± 0.5*	2.0 ± 0.3*	1.3 ± 0.2*
	Model B	8.1 ± 0.2	7.1 ± 0.5*	3.3 ± 0.3*	3.4 ± 0.4*
	Model C	7.2 ± 0.4	6.2 ± 0.5*	2.3 ± 0.2*	2.0 ± 0.1*
	Model D	6.7 ± 1.1	4.7 ± 1.0*	2.1 ± 0.3*	1.5 ± 0.2*

MPF: Mean Power Frequency, FMF: First Minimum Frequency, SAL: Spectral Areas of the Low; SAH: Spectral Areas of the High, RR: Rerative Ratio (SAL/SAH); Model A: an incision the right pars interarticularis, Model B: an incision the left pars interarticularis; Model C: an incision the right pedicle, Model D: an incision the left pedicle; *: vs. intact, $p < 0.01$.

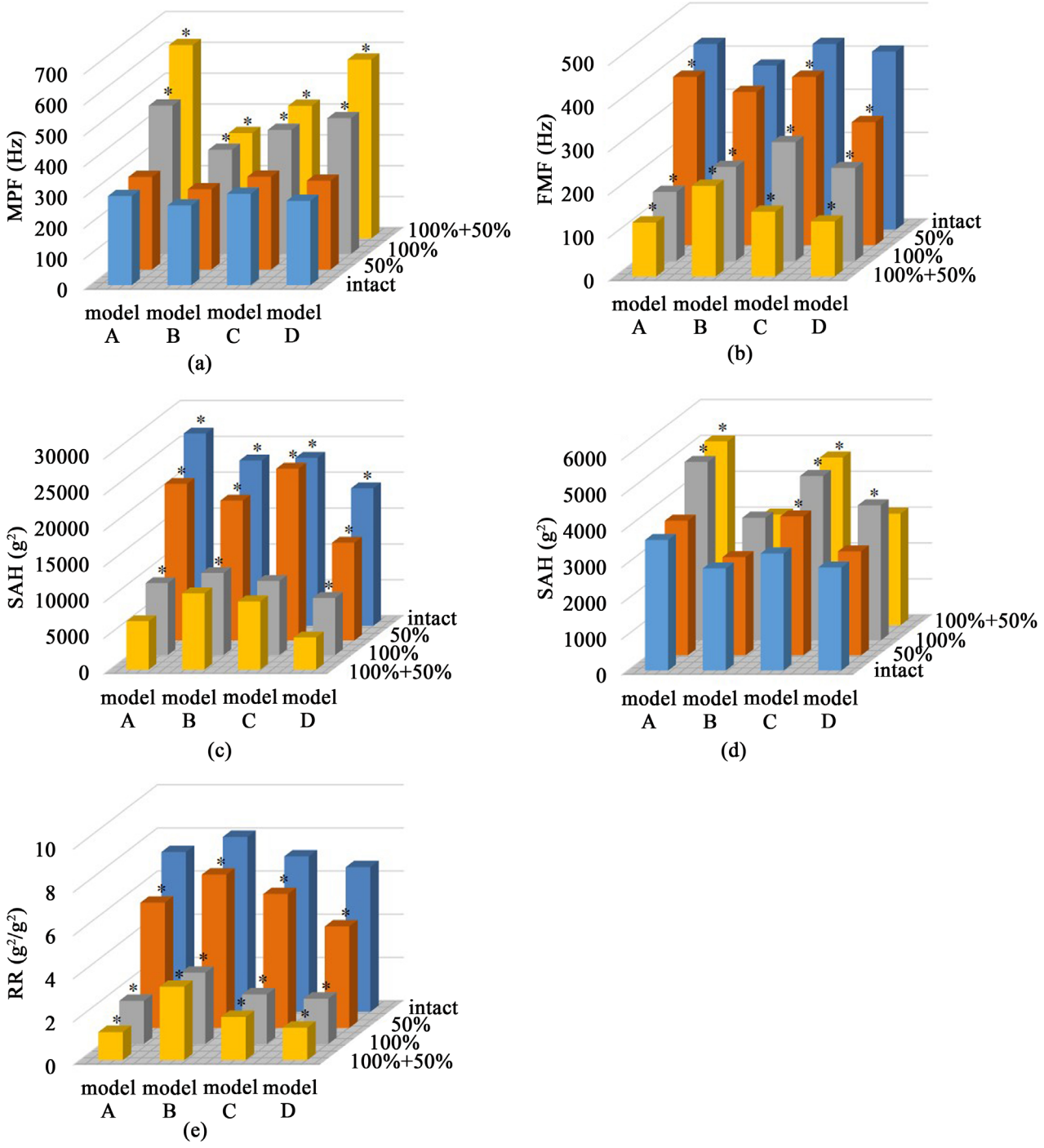

Figure 5. Results of analysis for each frequency parameter. For MPF and SAH, values are shown in the opposite order ("intact", "50%", "100%" and "50% + 100%") from that of FMF, SAL, and RR. (a) MPF (mean power frequency); (b) FMF (first minimum frequency); (c) SAL (spectral areas of the low); (d) SAH (spectral areas of the high); (e): RR (relative ratio (SAL/SAH)). *: vs. Intact, $p < 0.01$.

FMF (first minimum frequency)

Table 1 and Figure 5(b) show the values of FMF in the intact, 50%, 100%, and 100% + 50% incision conditions for models A, B, C and D: (model A) 430.0 ± 11.5 Hz, 390.0 ± 11.5 Hz, 160.0 ± 21.2 Hz, 125.0 ±

28.9Hz; (model B) 380.0 ± 25.8 Hz, 355.0 ± 10.0 Hz, 217.5 ± 9.6 Hz, 210.0 ± 87.0Hz; (model C) 430.0 ± 11.5 Hz, 390.0 ± 20.0 Hz, 275.0 ± 10.0 Hz, 150.0 ± 11.5Hz; (model D) 412.5 ± 45.0 Hz, 285.0 ± 44.3 Hz, 215.0 ± 10.0 Hz, 127.5 ± 23.6Hz. Compared to the intact condition, the values of FMF were significantly lower in the 50%, 100%, and 100% + 50% incision conditions for models A, C, and D, and in the 100% and 50% + 100% incision conditions for model B.

SAL (spectral areas of the low)

Table 1 and Figure 5(c) show the values of SLA in the intact, 50%, 100%, and 100% + 50% incision conditions for models A, B, C and D: (model A) 26,816.0 ± 2204.4 g^2, 21,829.3 ± 1563.0 g^2, 10,040.9 ± 759.1 g^2, 6759.8 ± 1029.7 g^2; (model B) 23,050.8 ± 765.3 g^2, 19,500.3 ± 679.4 g^2, 11,431.5 ± 1587.3 g^2, 10,638.5 ± 978.6 g^2; (model C) 23,427.5 ± 1412.2 g^2, 23,953.8 ± 2045.7 g^2, 10,337.5 ± 1246.6 g^2, 9518.6 ± 152.8 g^2; (model D) 19,185.8 ± 1136.5 g^2, 13,626.5 ± 1075.2 g^2, 7969.1 ± 580.3 g^2, 4500.0 ± 347.9 g^2. Compared to the intact condition, the values of SAL were significantly lower in the 50%, 100% and 100% + 50% incision conditions for models A, B, and D, and in the 100% and 100% + 50% incision conditions for model C.

SAH (spectral areas of the high)

Table 1 and Figure 5(d) show the values of SAH in the intact, 50%, 100%, and 100% + 50% incision conditions for models A, B, C and D: (model A) 3640.2 ± 402.5 g^2, 3755.2 ± 326.8 g^2, 4972.8 ± 163.4 g^2, 5124.9 ± 752.3 g^2; (model B) 2844.0 ± 118.1 g^2, 2738.7 ± 87.3 g^2, 3417.8 ± 311.7 g^2, 3084.4 ± 154.8 g^2; (model C) 3263.0 ± 268.8 g^2, 3875.7 ± 213.8 g^2, 4580.9 ± 460.5 g^2, 4675.9 ± 156.2 g^2; (model D) 2872.1 ± 283.6 g^2, 2900.5 ± 255.2 g^2, 3763.4 ± 332.5 g^2, 3110.8 ± 323.7 g^2. Compared to the intact condition, the values of SAH were significantly higher in the 100% and 100% + 50% incision conditions for model A, in the 50%, 100%, and 100% + 50% incision conditions for model C, and in the 100% + 50% incision condition for model D.

RR (relative ratio of spectral areas; SAL/SAH)

Table 1 and Figure 5(e) show the values of RR in the intact, 50%, 100%, and 100% + 50% incision conditions for models, A, B, C and D: (model A) 7.4 ± 0.5, 5.8 ± 0.5, 2.0 ± 0.3, 1.3 ± 0.2; (model B) 8.1 ± 0.2, 7.1 ± 0.5, 3.3 ± 0.3, 3.4 ± 0.4; (model C) 7.2 ± 0.4, 6.2 ± 0.5, 2.3 ± 0.2, 2.0 ± 0.1; (model D) 6.7 ± 1.1, 4.7 ± 1.0, 2.1 ± 0.3, 1.5 ± 0.2. Compared to the intact condition, the values of RR in the 50%, 100%, and 100% + 50% incision conditions were significantly lower for all models.

5. DISCUSSION

Vibration signal analysis system

Previous studies have used vibration signal analysis to identify fractures in long bones, such as the femur, tibia, and fibula [16-18]. In the vibration signal analysis of long bones, vibrational stimulation is applied to the distal end of the bone to detect the propagating signal from the proximal end [13]. That is, the presence or absence of fracture is determined from the attenuation of the intensity of the propagating signal from the distal end to the proximal end of the bone following vibrational stimulation. In the case of unilateral lumbar spondylolysis, however, vibration signals propagate from the intact lamina, so the attenuation of signal intensity is difficult to evaluate quantitatively. Therefore, in the present study, we constructed a qualitative evaluation system to measure changes in bone physical properties due to fractures. When an external force is applied to the bone, either elastic deformation, plastic deformation, or fracture deformation occurs, according to Young's modulus of the bone and the magnitude of the external force. The relationship between bone and force is represented by a stress-strain curve [19]. Since fractures reduce Young's modulus and decrease the natural frequency of bone, not only the measurement of signal intensity attenuation but also qualitative evaluation by frequency analysis can be useful for determining the presence or absence of fractures [20]. Therefore, it is reasonable to suppose that this method is more effective than the fracture evaluation by the conventional vibration signal analyse [21]. Moreover, our analysis system consisting of an amplifier, AD converter, and personal computer weighs less than 10 kg and is easy to set up. Thus, this system can be used in athletic fields where medical imaging cannot be performed.

MPF

The values of MPF were significantly increased in the 100% and 100% + 50% incision conditions compared to the intact condition. Campoli *et al.* [22] reported that bone shape and density influence the natural frequency of bone. Singh *et al.* [23] also investigated changes in the natural frequency of healthy and fractured bones and reported that the fractured bone had a low natural frequency. In the present study, both FMF and SAL values decreased with the severity of incision conditions. Therefore, the attenuation of the power in the low frequency area might have led to an increase in the high frequency area, resulting in the increase in MPF with increasing incision severity.

FMF, SAL, SAH, and RR

The values of FMF, SAL, and SAH significantly differed between the 100% and 100% + 50% incision conditions and the intact condition. Part of the 50% incision condition showed a significant difference from the intact condition. The results of the present study revealed a tendency to change greatly at 100% incision condition or more severity.

Since the continuity of the bone remained in the 50% incision condition, we consider that the vibration signal was transmitted through the bilateral vertebral arch. On the other hand, Young's modulus was also likely to be greatly influenced by the change in bone physical properties in the incision condition of 100% or more. In particular, RR showed high sensitivity, and values differed significantly between the intact condition and all incision conditions. In order to differentiate using more than two parameters, this method requires patients to have at least unilateral spondylolysis with a complete rupture (*i.e.*, more than 100% incision condition). However, to increase the possibility of fracture union, it is important to differentiate early-stage spondylolysis from other fractures. To this end, future investigation is warranted to improve frequency analysis methods for discriminating the 50% incision condition.

6. LIMITATIONS

The synthetic bone used in this study is made of a foam cortical shell. Since the natural frequency is affected by bone physical properties, the actual bone frequency properties may differ from the results of this study. Moreover, the present study did not take into consideration the effects of soft tissues such as ligaments and muscles. Tsuchikane *et al.* [24] investigated the effects of joints and soft tissues on the natural frequency of the human tibia and found that the natural frequency of the bone was affected by the mass of soft tissues attached to the bone. In the future, a review of bone-related studies and the influence of soft tissues on vibration signals will be necessary.

7. CONCLUSION

Lumbar spondylolysis models were created using synthetic bone to perform a frequency analysis of vibration signals. The spondylolysis models had three types of incisions (50%, 100%, and 50% + 100%) in the right or/and left pars interarticularis and pedicle. In the 100% and 50% + 100% incision conditions, a significant difference was observed in each parameter compared to the intact condition. Only RR showed a significant difference between the intact condition and all 50% incision conditions. Frequency analysis of vibration signals by spinous hammering could be useful in identifying lumbar spondylolysis.

ACKNOWLEDGEMENTS

This work was supported by JSPS KAKENHI Grant Number JP16K01771.

CONFLICTS OF INTEREST

The authors declare no conflicts of interest regarding the publication of this paper.

REFERENCES

1. Schroeder, G.D., LaBella, C.R., Mendoza, M., Daley, E.L., Savage, J.W., Patel, A.A. and Hsu, W.K. (2016) The

Role of Intense Athletic Activity on Structural Lumbar Abnormalities in Adolescent Patients with Symptomatic Low Back Pain. *European Spine Journal*, **25**, 2842-2848. https://doi.org/10.1007/s00586-016-4647-5

2. Sairyo, K., Katoh, S., Komatsubara, S., Terai, T., Yasui, N., Goel, K.V. and Ebraheim, N. (2005) Spondylolysis Fracture Angle in Children and Adolescents on CT Indicates the Facture Producing Force Vector: A Biomechanical Rationale. *The Internet Journal of Spine Surgery*, **1**, 2-7.
3. Sakai, T., Yamada, H., Nakamura, T., Nanamori, K., Kawasaki, Y., Hanaoka, N. and Sairyo, K. (2006) Lumbar Spinal Disorders in Patients with Athetoid Cerebral Palsy: A Clinical and Biomechanical Study. *Spine*, **31**, E66-E70. https://doi.org/10.1097/01.brs.0000197650.77751.80
4. Micheli, L.J. and Wood, R. (1995) Back Pain in Young Athletes. Significant Differences from Adults in Causes and Patterns. *Archives of Pediatrics & Adolescent Medicine*, **149**, 15-18. https://doi.org/10.1001/archpedi.1995.02170130017004
5. McTimoney, C.A.M. and Micheli, L.J. (2003) Current Evaluation and Management of Spondylolysis and Spondylolisthesis. *Current Sports Medicine Reports*, **2**, 41-46. https://doi.org/10.1249/00149619-200302000-00008
6. Lawrence, J.P., Greene, H.S. and Grauer, J.N. (2006) Back Pain in Athletes. *The Journal of the American Academy of Orthopaedic Surgeons*, **14**, 726-735. https://doi.org/10.5435/00124635-200612000-00004
7. Overley, S.C., McAnany, S.J., Andelman, S., Kim, J., Merrill, R.K., Cho, S.K. and Hecht, A.C. (2018) Return to Play in Adolescent Athletes with Symptomatic Spondylolysis without Listhesis: A Meta-Analysis. *Global Spine Journal*, **8**, 190-197. https://doi.org/10.1177/2192568217734520
8. Mushtaq, R., Porrino, J. and Guzmán Pérez-Carrillo, G.J. (2018) Imaging of Spondylolysis: The Evolving Role of Magnetic Resonance Imaging. *The Journal of Injury, Function, and Rehabilitation*, **10**, 675-680. https://doi.org/10.1016/j.pmrj.2018.02.001
9. Kalichman, L., Kim, D.H., Li, L., Guermazi, A., Berkin, V. and Hunter, D.J. (2009) Spondylolysis and Spondylolisthesis: Prevalence and Association with Low Back Pain in the Adult Community-Based Population. *Spine*, **34**, 199-205. https://doi.org/10.1097/BRS.0b013e31818edcfd
10. Goda, Y., Sakai, T., Sakamaki, T., Takata, Y., Higashino, K. and Sairyo, K. (2014) Analysis of MRI Signal Changes in the Adjacent Pedicle of Adolescent Patients with Fresh Lumbar Spondylolysis. *European Spine Journal*, **23**, 1892-1895. https://doi.org/10.1007/s00586-013-3109-6
11. Ganiyusufoglu, A.K., Onat, L., Karatoprak, O., Enercan, M. and Hamzaoglu, A. (2010) Diagnostic Accuracy of Magnetic Resonance Imaging versus Computed Tomography in Stress Fractures of the Lumbar Spine. *Clinical Radiology*, **65**, 902-907. https://doi.org/10.1016/j.crad.2010.06.011
12. Sairyo, K., Katoh, S., Takata, Y., Terai, T., Yasui, N., Goel, V.K. and Ebraheim, N. (2006) MRI Signal Changes of the Pedicle as an Indicator for Early Diagnosis of Spondylolysis in Children and Adolescents: A Clinical and Biomechanical Study. *Spine*, **31**, 206-211. https://doi.org/10.1097/01.brs.0000195161.60549.67
13. Mugunthan, K., Doust, J., Kurz, B. and Glasziou, P. (2014) Is There Sufficient Evidence for Tuning Fork Tests in Diagnosing Fractures? A Systematic Review. *BMJ Open*, **4**, 1-6. https://doi.org/10.1136/bmjopen-2014-005238
14. Kwatny, E., Thomas, D.H. and Kwatny, H.G. (1970) An Application of Signal Processing Techniques to the Study of Myoelectric Signals. *IEEE Transactions on Bio-Medical Engineering*, **17**, 303-313. https://doi.org/10.1109/TBME.1970.4502758
15. Baniqued, A.N., Zuniga, J.M., Strunc, T.C., Keenan, K.M., Boken, A.K. and Anderson, J.J. (2016) The Effect of Skinfold on the Assessment of the Mean Power Frequency at the Fatigue Threshold. *International Journal of Exercise Science*, **9**, 376-383.
16. Bache, J.B. and Cross, A.B. (1984) The Barford Test. A Useful Diagnostic Sign in Fractures of the Femoral Neck.

The Practitioner, **228**, 305-308.

17. Moore, M.B. (2009) The Use of a Tuning Fork and Stethoscope to Identify Fractures. *Journal of Athletic Training*, **44**, 272-274. https://doi.org/10.4085/1062-6050-44.3.272
18. Lesho, E.P. (1997) Can Tuning Forks Replace Bone Scans for Identification of Tibial Stress Fractures? *Military Medicine*, **162**, 802-803. https://doi.org/10.1093/milmed/162.12.802
19. McElhaney, J.H. (1966) Dynamic Response of Bone and Muscle Tissue. *Journal of Applied Physiology*, **21**, 1231-1236. https://doi.org/10.1152/jappl.1966.21.4.1231
20. Sylvester, A.D. and Kramer, P.A. (2018) Young's Modulus and Load Complexity: Modeling Their Effects on Proximal Femur Strain. *Anatomical Record*, **78**, 1-12.
21. Toney, C.M., Games, K.E., Winkelmann, Z.K. and Eberman, L.E. (2016) Using Tuning-Fork Tests in Diagnosing Fractures. *Journal of Athletic Training*, **51**, 498-499. https://doi.org/10.4085/1062-6050-51.7.06
22. Campoli, G., Baka, N., Kaptein, B.L., Valstar, E.R., Zachow, S., Weinans, H. and Zadpoor, A.A. (2014) Relationship between the Shape and Density Distribution of the Femur and Its Natural Frequencies of Vibration. *Journal of Biomechanics*, **47**, 3334-3343. https://doi.org/10.1016/j.jbiomech.2014.08.008
23. Singh, V.R., Yadav, S. and Adya, V.P. (1989) Role of Natural Frequency of Bone as a Guide for Detection of Bone Fracture Healing. *Journal of Biomedical Engineering*, **11**, 457-461. https://doi.org/10.1016/0141-5425(89)90039-3
24. Tsuchikane, A., Nakatsuchi, Y. and Nomura, A. (1995) The Influence of Joints and Soft Tissue on the Natural Frequency of the Human Tibia Using the Impulse Response Method. *Proceedings of the Institution of Mechanical Engineers. Part H, Journal of Engineering in Medicine*, **209**, 149-155. https://doi.org/10.1243/PIME_PROC_1995_209_337_02